14th Asia-Pacific Conference on Combustion
Kaohsiung Exhibition Center, Kaohsiung, Taiwan
14th-18th May 2023

Experimental Spray Characterization for Jet-A1 Under Temperature Controlled Subcritical, Transcritical, and Supercritical Spray Conditions

Kaushik Nonavinakere Vinod[1], Robert Kempin[1], Tiegang Fang[1*]

[1]Dept. Of Mechanical and Aerospace Engineering, North Carolina State University

1840 Entrepreneur Drive, Raleigh, North Carolina, 27695, USA

Abstract

Fuels when sprayed under superheated and elevated fuel pressure show different behavior than traditional fuel injection sprays. In this work optical diagnostics were used to study the behavior of Jet A-1 under subcritical, transcritical, and supercritical sprays into open air ambience. Five different temperatures were tested, and the resultant spray images were processed to obtain quantitative measurements such as spray penetrations, and spray cone angle for each case. The spray structure transition with changing parameters from subcritical, transcritical, and supercritical states were also studied. The transition between the three different states are shown in this study and the resulting spray cone angles and penetrations are compared for the fuel. The results show that a transcritical spray has a measurable variation in the spray cone formation and penetration process for a fixed injection pressure. At this state the spray cone shows a bimodal spray angle relationship with increasing penetration. Flash boiling of the fuel is observed near the nozzle of the injector. Increasing the temperature further into the supercritical regime, the spray plume shows a thinning of the jet near the nozzle with a reduced overall penetration compared to lower temperatures.

1 Introduction

With recent developments in automobile propulsion technologies there is huge focus on improving the efficiency and emission characteristics of the internal combustion engine (ICE) [1]. The unparalleled energy density, relative ease of manufacture. and fuel flexibility of an ICE makes it an essential energy source for the foreseeable future. Increasing strictness of emission control combined with the recent developments in finding alternative and “clean” fuels have created a need for the ICE to adapt and employ new technologies and several optimizations to existing technologies [2].

Optimizations to the fuel delivery systems like gasoline direct injection (GDI), and spark assisted compression ignition (SACI) have shown to improve both fuel efficiency and reduce overall NO_x and CO_2 engine out emissions while improving engine performance with traditional fossil fuels [3]. Optimizations to advanced fuel delivery systems and additions of forced inductions systems have created a recent focus shift to study the improvements in combustion quality based on new techniques in air-fuel mixing inside the combustion chamber [4].

One such new technique of great potential is supercritical and transcritical spray combustion [5,6,7]. Recently, high pressure fuel injections in the order of 400 to 500 bar have been widely used to improve the combustion quality. Studies shows that further increase in operating pressure of the fuel system can benefit the fuel atomization process by generating finer droplets which can help reduce emissions and improve combustion quality [8,9,10]. However, there is an inverse correlation between increasing the fuel pressure and the cost of application. Supercritical and transcritical fuel injection systems can thus be beneficial for improving system cost effectiveness. With a supercritical spray, the fuel being sprayed will have better evaporation, atomization, dispersion, and diffusion than that of a subcritical high pressure injection system. Since the density of a supercritical fluid is relatively higher, the cost of fuel delivery can be optimized for the relative performance gains [11,12,13].

A fuel spray can be considered supercritical if the fuel in the injector before injection has the temperature and pressure above the critical point of the fuel. Several studies have been performed showing the effect of hydrocarbon based fuels at supercritical state being sprayed into a subcritical atmosphere [14]. Studies performed with the fuel heated and pressurized beyond the supercritical point in a gasoline direct injection system (GDI) show that there can be reductions in particulate matter emissions in the engine exhaust which could be caused by the improved fuel atomization and reduced mean droplet size of the spray [15].

While studies involving supercritical sprays have focused on characterizing the droplet diameter under a selected temperature and pressure, few studies show the effect of supercritical spray on the spray plume generated after injection. Understanding the changes in the spray plume can be beneficial in designing combustion chambers and injector nozzles for better atomization. Moreover, the transition state between subcritical and supercritical states, called the transcritical state, is of great interest as it can be achieved more reliably with very little modifications to existing high pressure fuel systems and can provide benefits in atomization of fuel due to flash boiling effects of the fuel but at elevated temperatures.

In this work, several different fuel sprays ranging from subcritical to supercritical states before injection were characterized using high speed imaging. Jet A-1 was used as the fuel for this study due to its atomization properties. A single hole diesel injector was used with a custom heater and injected into ambient atmospheric conditions. The penetration lengths and spray angle were studied to characterize the different sprays.

2 Experimental Setup

For this study a single hole high pressure diesel injector was used to spray fuel. The injector has a nozzle diameter of 200 µm and is controlled by a custom injector driver. The injector is placed inside a heater block and is secured with fasteners. The heater block is fitted with two 500 W heaters. The heaters can heat the

*Corresponding author,
E-mail address: tfang2@ncsu.edu

whole injector up to 650 K. The fuel is pressurized using a high-pressure air driven pump capable of generating 420 MPa. The pressure and the temperature of the injector were controlled by a closed loop controllers to ensure accurate and repeatable settings. For this study four different temperatures at a pressure of 150 MPa were tested. The injector was suspended in an open-air test cell maintained at a temperature of 297 K at atmospheric pressure. The resulting spray from the injector was recorded using a Phantom VEO 710 high speed camera. The spray was backlit using a diffused LED light source. The injector driver was synced to the camera trigger ensuring repeatable synchronization. Figure 1 shows a schematic of the experimental setup. The fuel lines leading to the injector were also heated using a strip heater to 390 K to ensure the fuel inside the injector can have a stable temperature even when there is flow inside the fuel return from the injector to the fuel tank. At the beginning of every experiment the pump is activated to pressurize the injector while the heater is commanded to heat the injector block to the set temperature. Once the temperature is reached, the system is left idle to reach an equilibrium. After that the injector is triggered to spray and the cameras are triggered to record the images and the system is reset for the next experiment. Table 1 shows the experimental conditions tested in this study. Due to the small fuel quantity injected, it is expected that the fuel temperature in the nozzle is similar to the injector nozzle temperature.

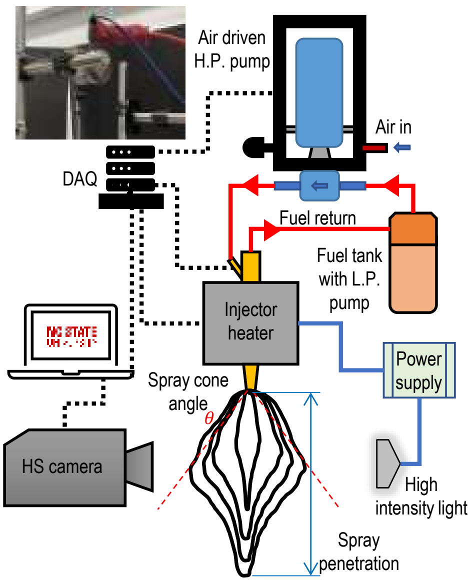

Figure 1: Experimental setup used for testing showing the spray measurement techniques.

Table 1: Experimental conditions tested.

Experimental conditions	Value
Fuel	Jet-A1
Fuel rail pressure	150 MPa
Injector nozzle temperature	423 K, 473 K, 528 K, 548 K, 573 K

3 Results and Discussion

Data from the high-speed camera was processed in custom Matlab and ImageJ code to generate spray contours after removing the background. Using the spray contours the spray penetration and spray cone angle values were calculated for each case tested. Following sections discuss the data recorded in detail.

3.1 High Speed Spray Images

Figure 2 shows a sequence of spray images for three nozzle temperatures with increasing time after injection was triggered. The three temperatures were chosen to showcase the three different regimes of the fuel spray. 423 K shows the subcritical spray, 548 K for the spray at transcritical conditions, and 573 K spray can be used to represent a supercritical spray.

Looking at the three temperatures at early stages of the injection there is a noticeable difference in the fuel spray jet exiting the nozzle. With the temperature increasing there is a change in the profile of the fuel spray. The effect of fuel flash boiling at the transcritical and supercritical states can also be seen around the jet.

After the initial jet has exited the nozzle, the spray development is affected by the change in the flash boiling effect between the different states. The low temperature/subcritical spray shows a relatively normal spray development with the spray containing mainly liquid droplets that are carried out by the pressure of injection. The transcritical spray shows a central narrow liquid jet surrounded by a plume of fast vaporizing fuel. With the 573 K case there is only a narrow central jet that is made up of a small quantity of liquid that is propelled by the pressure of injection. Around the central jet we can see a rapidly diffusing plume of fuel caused by the fuel being nearly in the supercritical state.

With further increase in time, since the fuel in the transcritical state will lose temperature to the ambient it no longer shows rapid expansion like the supercritical spray. The transcritical spray returns to developing a spray that looks more like a subcritical fuel spray jet. However, there is still a small section near nozzle (up to around 2 mm from the nozzle tip) that shows flash boiling effects for as long as the injector stays open. The supercritical spray, however, shows a bimodal operation with the first ~2-4 mm showing a relatively narrow jet and a sudden increase in the plume width afterwards displaying increased turbulence caused by the fuel rapidly diffusing and vaporizing. The initial narrow jet can be explained by the fuel jet being driven by the inertia provided by the pressure of injection and the quick change in the spray width can be explained by the fuel rapidly boiling and diffusing as the temperature of the fuel should still be relatively close to or above the critical temperature of the fuel.

3.2 Spray Cone Angle

Figure 3 shows the mean spray cone angle measured for all the sprays tested in this study. The inset inside Fig-3 shows an expanded view of the first 250 µs after triggering the injection event.

From Fig. 3 it is evident that with increasing fuel temperature there is a noticeable change in the mean spray cone angle with all other conditions maintained constant. All the sprays tested show an increased spray angle right after the start of injection and a drop with eventual plateauing of the spray cone angle. With increasing fuel temperature this effect is exaggerated and the sprays show a bimodal variation in the cone angle development. Both 548 K and the 573 k cases show a spray that has a wider spray cone for longer. This could be due to the initially hot fuel

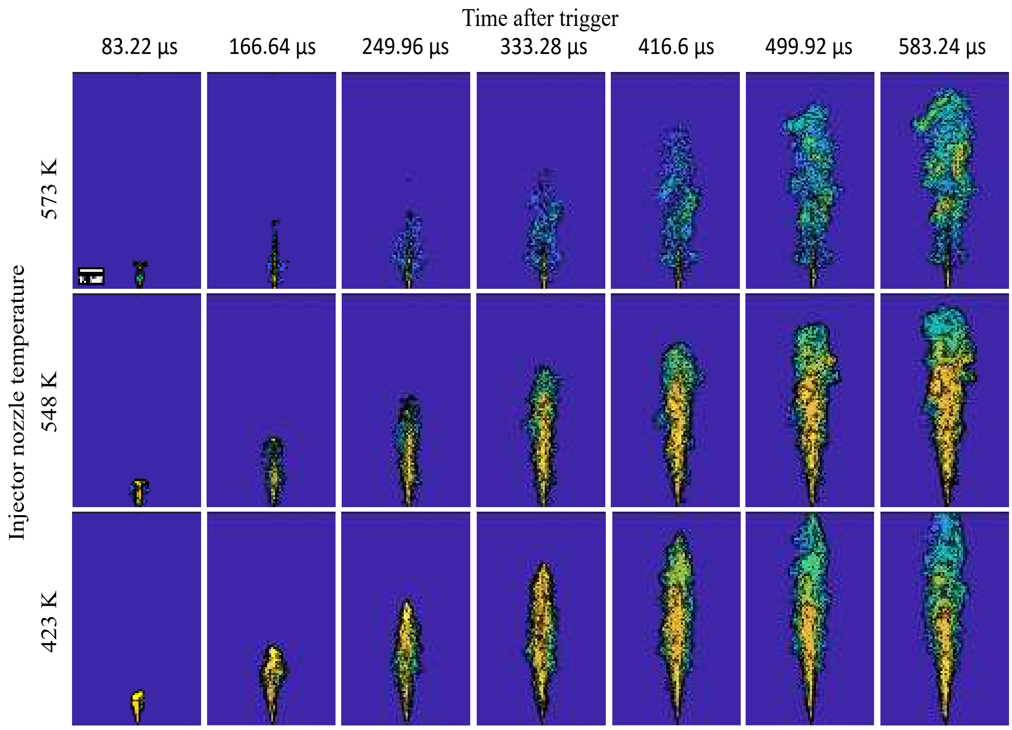

Figure 2: High speed image contours of three different temperatures showing subcritical, transcritical, and supercritical fuel injections over time.

from the injector diffusing into the atmosphere quickly as the fuel would be closer to transcritical/supercritical conditions. As the fuel is injected out, the temperature of the fuel inside the injector will drop slightly causing the effect of instant diffusion and flash boiling to reduce and settle into a balance causing the slight second increase in the cone angle before plateauing.

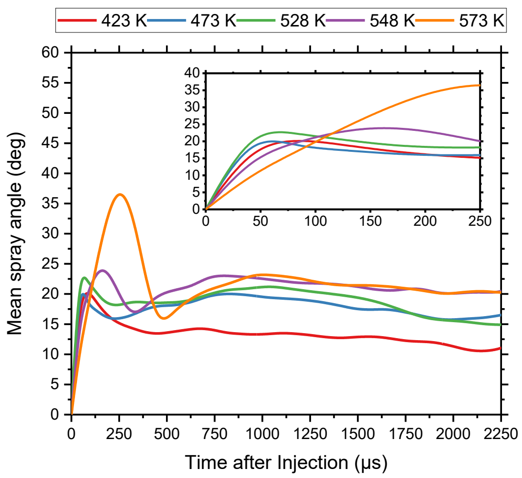

Figure 3: Mean spray cone angle measurements for all the sprays tested with the inset figure showing the initial 250 µs of the spray after injection was triggered.

From Fig. 3 it is also evident that the extent of the fuel being closer to the critical temperature has a considerable effect in how fast the fuel can vaporize. With just a 25 K increase in temperature from 548 K to 573 K the spray shows a 50% increase in the cone angle.

3.3 Spray Penetration

Using the high speed images, we can calculate the spray penetration overtime for all the sprays tested. This gives us an understanding of how the spray is affected by the rapid diffusion caused by the increased temperatures or the fuel changing states before injection. Fig. 4 shows the spray penetration over time after the start of injection for these different temperatures. Because of how the camera and image capture was setup and the high pressures of the experiment the spray jets show penetration beyond the field of view of the cameras after a certain time. This distance is depicted by a dotted line at 121 mm in Fig. 4.

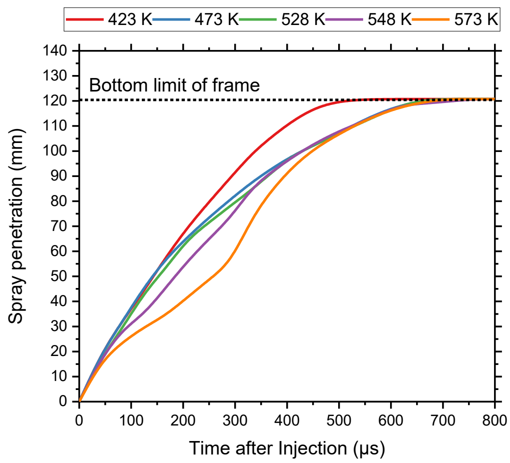

Figure 4: Spray penetration with time for all the cases tested.

From Fig. 4 it is evident that there is a reduction in the rate of penetration with increasing temperature. This is caused by the fuel diffusing radially around the spray jet in the initial stages of injection due to fuel being transcritical/supercritical. At 423 K the fuel spray shows a relatively linear penetration rate with time. With the temperatures increasing to the transcritical temperatures for Jet-A1, there is a reduction in the penetration quickly after the injection starts. This is caused by the rapid boiling and diffusion of the fuel as noticed in the cone angle measurements. With fuel state being closer to the supercritical temperature of the fuel the initial penetration is substantially reduced. But this reduction in penetration is accompanied by the increase in spray diffusion and boiling, thus improving the vaporization and atomization characteristics of the fuel.

Using the data from Fig. 4, we can calculate the speed of penetration of the different sprays as shown Fig. 5.

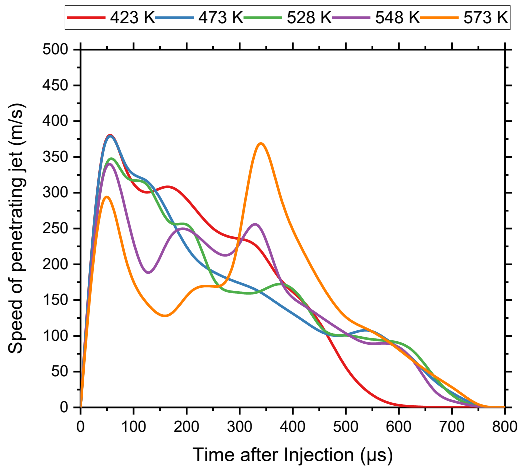

Figure 5: Spray penetration speed measurements for all the cases tested.

From Fig. 5, at lower temperatures (subcritical states) the fuel spray displays a high speed of penetration in the initial stages of the spray development. This can be explained by the relatively high concentrations of liquid fuel being propelled out of the nozzle by the pressure of injection with low diffusion or vaporization. As the temperature increases, we see a reduction in the speed as the effect of injection pressure is subdued by the reduction in the liquid fuel fraction in the spray jet. The increased vaporization/boiling and diffusion caused by the fuel being in a transcritical/supercritical state caused the slow penetration speed as larger quantities of fuel vaporizes radially around the spray jet. With increasing time, as the fuel inside the heated injector will be reduced in temperature due to the process of being injected the jet will start to penetrate faster as shown by the increase in the spray penetration speed.

4 Conclusions

In this study Jet-A1 fuel sprays are characterized for subcritical, transcritical, and supercritical spraying regimes. Optical diagnostics by the means of backlit shadowgraphy was used to capture the spray jets in high speed and the resulting spray cone angle, spray penetration and spray penetration speeds are measured. Five different temperatures of the fuel were studied under an injection pressure of 150 MPa. Following are some key points of the study:

- Increasing the temperature from subcritical to supercritical states shows a measurable change in the liquid-vapor concentrations in the spray jet. This reduction in the liquid phase allows the jet to have a wider cone angle. This effect is also amplified by increased vaporization and boiling.
- The spray under supercritical conditions shows two modes of dispersion, an initial pressure driven mode where a narrow column of hot liquid is propelled by the injection pressure and a diffusion driven expansion where the near supercritical fuel from the jet diffuses and boils.
- The spray cone angle measurements also show the same bimodal trend with increasing temperature. The effect is amplified with temperatures near and in excess of the supercritical temperature of the fuel.
- With increasing temperatures, there is a sacrifice in spray penetration length and the speed of penetration as there is a reduction in liquid concentrations in the spray jet with fuel temperatures in transcritical or supercritical regimes.

5 Acknowledgment

This material is based upon work supported by, or in part by the National Science Foundation under Grant No. CBET- 2104394. Any opinions, findings, and conclusions or recommendations expressed in this material are those of the author(s) and do not necessarily reflect the views of the funding agencies.

References

• Lešnik, L., Kegl, B., Torres-Jiménez, E. and Cruz-Peragón, F., Oil & Gas Science and Technology–Revue d'IFP Energies nouvelles, (75) (2020) 56.

• Lu, X., Han, D. and Huang, Z., Progress in Energy and Combustion Science 37(6) (2011) 741-783.

• Qian, Y., Li, H., Han, D., Ji, L., Huang, Z., & Lu, X. Energy, (111) (2016) 1003-1016.

• Lee, K., Cho, S., Kim, N. and Min, K., Energy, (91) (2015) 1038-1048.

• Anitescu, G., Bruno, T.J. and Tavlarides, L.L., Energy & fuels, 26(10) (2012) 6247-6258.

• Zhu, H., Battistoni, M., Ningegowda, B.M., Rahantamialisoa, F.N.Z., Yue, Z., Wang, H. and Yao, M., Fuel, (307) (2022) 121894.

• Chung, W.T., Ma, P.C. and Ihme, M., International Journal of Engine Research, 21(1) (2020) 122-133.

• Morgan, R., Banks, A., Auld, A. and Heikal, M., (No. 2015-24-2441) (2015) SAE Technical Paper.

• Wang, L., Lowrie, J., Ngaile, G. and Fang, T., Applied Thermal Engineering, (152) (2019) 807-824

• Yao, C., Hu, J., Geng, P., Shi, J., Zhang, D. and Ju, Y., Fuel, (206) (2017) 593-602.

• Lacaze, G. and Oefelein, J.C., Combustion and Flame, 159(6) (2012) 2087-2103.

• Givler, S.D. and Abraham, J., Progress in Energy and combustion Science, 22(1) (1996)1-28.

• Li, L., Xie, M., Wei, W., Jia, M. and Liu, H., Cryogenics, (89) (2018) 16-28.

• Xia, J., Huang, Z., Xu, L., Ju, D. and Lu, X., Energy Conversion and Management, (195) (2019) 958-971.

• Fan, X., Yu, G., Li, J., Zhang, X. and Sung, C.J. Journal of Propulsion and Power, 22(1) (2006) 103-110.